Anisotropic responsive microgels based on the cholesteric phase of chitin nanocrystals

Sujin R. Lee,[a] Elsa Reichmanis,[*,b] and Mohan Srinivasarao[*,a,c]

[a]School of Chemistry and Biochemistry, Georgia Institute of Technology, Atlanta, GA, 30332

[c]School of Materials Science and Engineering, Georgia Institute of Technology, Atlanta, GA 30332

[b]Department of Chemical & Biomolecular Engineering, Lehigh University, Bethlehem, PA, 18015

*Corresponding author: mohan@mse.gatech.edu, elr420@lehigh.edu

Abstract

Anisotropic stimuli-responsive microgels based upon the cholesteric phase of chitin nanocrystals and N-isopropylacrylamide were designed and synthesized. The cholesteric structure was interrogated and the texture was shown to directly influence microgel shape and anisotropy. Changes in microgel volume led to changes in texture, where microgels comprising up to 6 bands exhibited a twisted bipolar texture while those with greater volumes displayed a concentric-packing structure. As designed, the imprinted cholesteric phase induced an asymmetric response to temperature, leading to a change in shape and optical properties. Furthermore, the cholesteric structure is able to deform, facilitating transport into a small channel. Access to synthetic structures having self-assembled twisted texture derived from cholesterics embedded within a polymer matrix will provide guidelines for designing biopolymer composites with programmable motion.

Introduction

Many biological materials, including fruit shells, leaves and the exoskeleton of arthropods (e.g., beetles), possess embedded hierarchical structures that lead to their structural integrity as well as their appearance.[1-6] Such structures consist of a multilayered and twisted microstructure, often termed as a "Bouligand Structure". The Bouligand structure comprises nanometric fibers, aligned uniaxially into planar sheets, which stack to form a helicoid. These structures are believed to offer a combination of high impact tolerance, high mechanical strength and stimuli responsive behavior such as that seen in fibrillar assemblies embedded within hydrogel matrices.[7] Thus, the exceptional properties of the Bouligand structure are often a source of inspiration for producing biomimetic high-impact resistant hydrogels that adapt to their surroundings.[7-10] Developing hydrogels with anisotropic swelling/deswelling, similar to that found in biological organisms is an important step towards realizing the full potential of synthetic systems. While anisotropic hydrogels have been demonstrated,[11-25] their fabrication protocols generally require multiple fabrication steps and/or 3D bioprinting systems.

The twisted structure associated with the "cholesteric" liquid crystal phase of cellulose and chitin nanocrystals (CNCs and ChNCs, respectively) is analogous to the "Bouligand Structure". Further, when embedded within a hydrogel matrix, synthetic hydrogels having properties similar to those found in nature could be envisioned.[26-34] They could serve as a template offering a simple, efficient method to generate an hierarchical, anisotropic internal structure obviating the need for complex and/or expensive fabrication methods.[35-38] For instance, when incorporated into isotropic hydrogels, rod-like viruses imparted an ordered structure whereby the composite exhibited anisotropic swelling.[35] Further, hydrogels using the cholesteric architecture of an aqueous

suspension of CNCs as a template have been achieved.[38-41] Nevertheless, reports of cholesteric templated hydrogels that exhibit *anisotropic* response to stimuli remain elusive.

Here, we design and interrogate anisotropic stimuli-responsive microgels based upon the ChNCs cholesteric phase and N-isopropylacrylamide (NIPAM). Size-controlled microgels were created upon emulsification of a mixture of NIPAM, self-assembled chitin suspension, a crosslinking agent and initiator in a microfluidic device. UV irradiation effected polymerization of NIPAM into a cross-linked poly(N-isopropylacrylamide) (pNIPAM) matrix. The ChNC cholesteric structure embedded within the hydrogel matrix was then characterized. The director configuration of the cholesteric phase changed with droplet dimension, and the microgels underwent anisotropic swelling when immersed in water, largely along the twist direction. The cholesteric structure dictated final microgel shape and response to external stimuli.

Result and Discussion

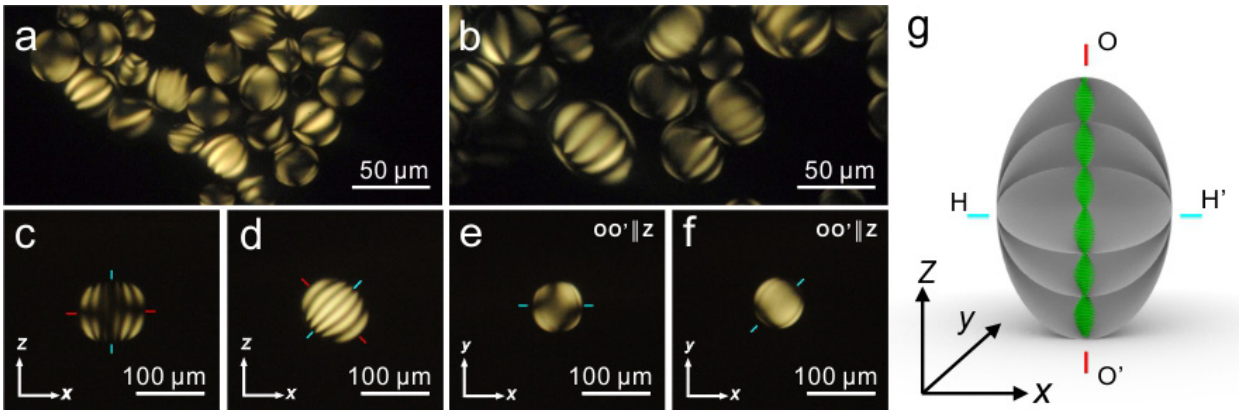

Figure 1. POM images of chitin microgels in (a) IPA, and (b) water. POM images of (c and d) of an individual microgel with 6 cholesteric bands with the OO′ and HH′ axes perpendicular to the y axis obtained at different angles; with axial views (e and f, where the OO′ axis is parallel to the z axis. The white arrows indicate the imaging planes. (g) Schematic of a microgel having twisted bipolar texture without considering the viewing direction.

An aqueous suspension of ChNCs was prepared by acid hydrolysis of chitin.[42-44] The suspension formed a cholesteric phase at pH 2 and above 2 wt % (see supplementary and Fig. S1-S4 for details). The ChNC cholesteric phase was mixed with NIPAM, cross-linker and photoinitiator. Subsequently, the solution was emulsified in a microfluidic device (Fig. S5) to generate ChNC-monomer droplets with an average diameter of 40 μm. Once formed, the droplets were stored for 48 hrs to generate well-aligned cholesterics (Fig. S6). Subsequent UV irradiation afforded microgel particles, comprising cholesteric structures embedded within crosslinked pNIPAM microgels. Polarized optical microscopy (POM) imaging verified that the cholesteric structure was preserved, and most gels contained 6 cholesteric bands (characteristic stripes, where double the distance between two adjacent band is the helical pitch) (Fig. 1a). Upon immersion into water for storage, the hydrophilic pNIPAM microgels expanded. The swelling was anisotropic: the major and minor axes changed by 210 % and 141 %, respectively, where the helical axis acts as the long axis. (Fig. 1b).

In the cholesteric droplet, a relative chirality parameter $N = 2d / p$ (d = the droplet diameter, p = the cholesteric pitch) defines the number of π turns of the director in a droplet, which can be used to evaluate the texture.[45, 46] For ChNC-pNIPAM, because of the anisotropic swelling, we used the number of cholesteric bands along the twist direction to explain observed morphologies. Individual microgels possessing 6 cholesteric bands were examined by rotating the structures under crossed polarizers. POM images of two common orientations of the microgel are provided in Fig. 1c-f. Fig. 1g shows the corresponding schematic of the ChNC microgel with pseudo-layers depicted as grey surfaces separated by half-pitch. By adopting a cartesian coordinate system, the z-axis was set parallel with the helical axis. The helical axis is marked as axis OO′. Axis HH′ intersects the twist axis perpendicular to the cholesteric planes in the droplet center. The microgel (Fig. 1c, d) shows

typical cholesteric structure in an elliptical shape having an aspect ratio of 1.33 when the OO′ and HH′ axes were perpendicular to the y-axis. A dark line crossing the center was observed when the microgel OO'-axis was aligned parallel to either the polarizer or analyzer (Fig. 1c). This texture is analogous to the twisted bipolar structure.

Fig. 1e, f are axial views of the microgels (OO' ∥ z) and can either represent the top or bottom of the cholesteric. In the twisted bipolar configuration, two surface point (boojum) defects should be located at the poles. However, from the poles of the microgels, bipolar nematic orientation-like texture was revealed. This observation is similar to simulations reported by de Pablo et al.,[45] who employed Landau–de Gennes (LdG) energy function and a tensorial order parameter to model cholesteric droplets. The director orientation in horizontal cross section of planar bipolar structure (one cholesteric plane) was predominantly uniform except for those near the surface. From the side and axial views, the current microgels have a prolate spheroid shape ($a \approx b < c$) (Fig. 1g). Bright field imaging confirmed that the cholesteric microgels were elongated along the helical axis (Fig. S7b). In contrast, microgels produced with the isotropic phase of the ChNC suspensions were spherical, with no cholesteric structure or birefringence (Fig. S7c).

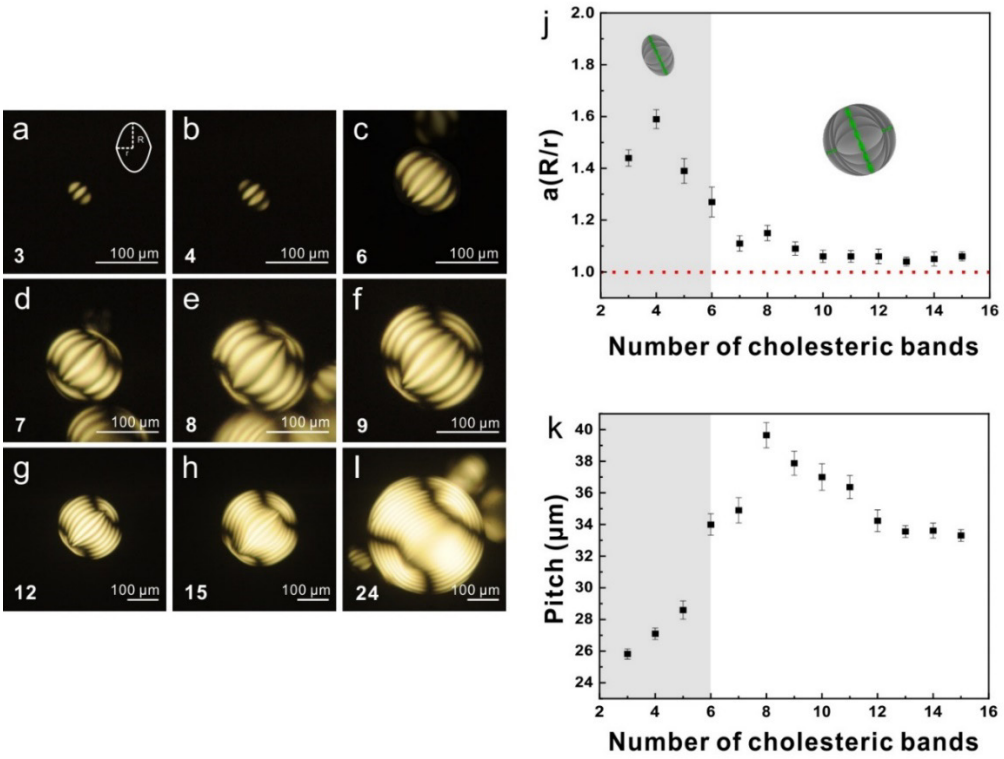

Figure 2. (a-i) POM images of chitin microgels with different number of cholesteric bands. (j) Aspect ratio of chitin microgel with corresponding number of cholesteric bands. (k) Pitch variation plotted as a function of number of cholesteric bands. For each data point, 20 microgels were analyzed. Grey color region in j and k indicates microgels having twisted bipolar structure.

To understand the effect of microgel size on the morphology and anisotropic nature of the cholesteric phase, we examined microgels with controlled numbers of stripes. Microgels having fewer than 2 bands were excluded since their helical twisting was not fully resolved. The structural transition observed in the droplets is primarily governed by the interplay between droplet elastic energy and surface anchoring energy.[47-50] The elastic energy can be scaled with droplet radius (~Kr). The one elastic constant approximation was used for simplicity, though the K_2 (twist) is often an order magnitude smaller than K_1 (splay) and K_3 (bend) for cholesteric biocolloids.[51, 52] The anchoring energy was scaled as Wr^2 where W is surface anchoring energy per unit area. When

r << K/W, the cholesteric droplet disturbs the boundary conditions and exhibits a twisted bipolar texture due to the large elastic energy. In the case of r >> K/W, the droplet is expected to adopt a concentric-packing structure, which satisfies the surface anchoring since the energy penalty associated with strain is low.[47-49] Examination of Fig. 2a-i suggests that the ordering of the cholesteric phase in ChNC microgels is driven by the surface anchoring and elastic energies. The aspect ratio of the microgels, plotted as a function of the number of cholesteric bands is presented in Fig. 2j. Microgels with less than 6 bands (major axis ≤ 100 μm) exhibited a twisted bipolar structure, which does not satisfy the planar anchoring condition (Fig. 2a-c). Due to asymmetric swelling in water, the structures were elongated with aspect ratios > 1.2. Microgels having 4 bands displayed the highest aspect ratio, namely 1.64 (Fig. 2j).

Increased microgel volume led to an anchoring energy induced change in cholesteric alignment from homeotropic to planar. When the volume was sufficiently high to accommodate > 7 cholesteric bands, bands with planar anchoring added perpendicularly to the twisted bipolar structure, resulting in reduction in microgel aspect ratio. (Fig. 2 d-f). Microgels larger than 120 μm (≥ 9 bands) appeared spherical, as more bands preferentially developed perpendicularly onto the twisted bipolar structure (Fig. 2g-i). Under these circumstances, the twisted ChNC structure behaved as a phase grating (see Supplementary Information and Fig. S8). Sufficiently large (≥ 14 bands) microgels had an aspect ratio near 1 and exhibited onion-like texture with concentric packing, satisfying the planar anchoring condition (Fig. 2i). The aspect ratio of the polar to equatorial length gradually decreased from 1.64 to 1.06 as the internal texture transformed from twisted bipolar to concentric-packing (Fig. 2j). Bright-field images (Fig. S9) confirm the dependence of microgel shape on inner structure. Microgels larger than 300 μm exhibited poor alignment (Fig. S10).

In a theoretical investigation that relied on tensorial description of the local order and LdG theory, Sleczkowski et al. revealed that the twist, close to the center of the cholesteric droplet elongates due to significant bend elastic deformation.[53] They observed an increase in pitch near the droplet center compared to the intrinsic cholesteric pitch in experimental and simulated data for thermotropic cholesteric droplets with radial spherical structure. Similarly, the cholesteric pitch in the microgels depend on internal structure coupled with dimension. The phenomenon is exemplified in Fig. 2d-f where the cholesterics are in an intermediate structural state, namely between twisted bipolar and concentric-packing: the pitch near the droplet center is expanded, affecting the mean pitch. For those microgels, the relative change of pitch in the center (p) to the mean pitch (p_i), defined as $(p - p_i)/p_i$, was 0.23, 0.32, and 0.34 for microgels having 7, 8 and 9 bands, respectively. As depicted in Fig. 2k, when the number of cholesteric bands increased from 3 to 8, microgel texture transformed from twisted bipolar to the intermediate structure, while mean pitch increased from 26 μm to 39 μm. For spherical microgels having concentric-packing (≥ 9 bands), the mean pitch decreased, gradually diminishing the elongation effect near the center. The mean pitch of the microgels with ≥ 14 bands was invariant at 34 μm.

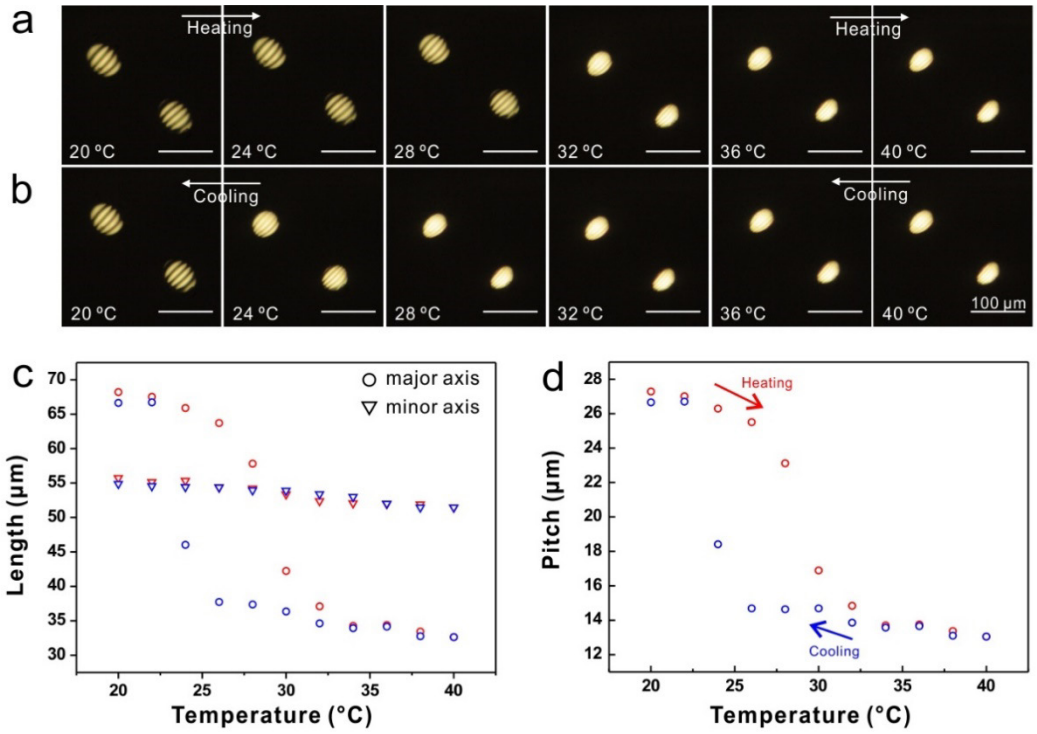

Figure 3. POM images of microgels with 5 bands at different temperatures during (a) heating and (b) cooling after 3 min equilibration time at each temperature. Effect of temperature on the (c) major, minor axis and (d) pitch during heating (red) and cooling (blue).

The lower critical solution temperature (LCST) of pNIPAM is 32 °C where polymer chain conformational changes lead to a temperature induced volume phase transition.[54, 55] These transitions are also expected to impact the ChNC microgels, and thus their thermo-response was evaluated. Microgels comprising 5 periodic bands were immersed in water, heated from 20 °C to 40 °C, and subsequently cooled to 20 °C. Fig. 3a, b demonstrates that microgel size changed inversely with temperature, with a sharp transition in the range of 28 to 32 °C. Fig. 3c presents the change in dimension of the major and minor axes upon heating/cooling. The thermo-responsive behavior was anisotropic; along the twist direction, increasing temperature led to decreased microgel length by about 52 %, whereas the change in minor axis length was limited to 8%. Fig. 3d shows the corresponding pitch as a function of temperature. In the fully 'swollen' state, the

cholesteric pitch was 26.9 µm. When the temperature increased above the LCST, the pitch decreased to 13.5 µm. As quantified using imageJ[56], at 40 °C microgel brightness was 50% higher than that at ambient temperature. On the axial view, microgel shrinkage was 10%, verifying the asymmetrical swelling (Fig. S11a, b). Thermo-responsive behavior of a concentric-packing microgel is shown in Fig. S11c, d. Spherical microgels also shrank parallel to the helical axis, changing shape from sphere to spindle. The response of the texture within the microgels in the presence of osmotic stress (Fig. S12) shows analogous response to thermal stimulus.

The asymmetric stimulus-response of the microgels shares similarities with modeling of the Bouligand structure of lobster cuticle.[57] The ratio of the structure's Young's modulus from the axial to transverse directions of the helix was calculated as 1.4. This anisotropy optimizes mechanical properties. In this regard, the anisotropic swelling of the ChNC microgels confirmed that the ChNC cholesteric phase is a promising route to impart Bouligand structural characteristics to a host matrix.

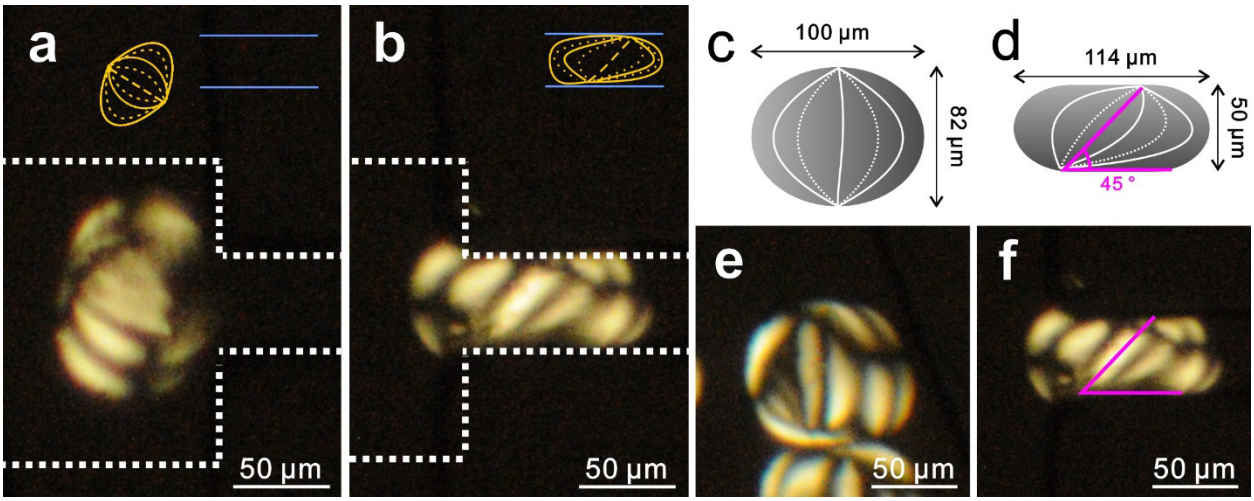

Figure 4. POM images of microgel with twisted bipolar configuration (a) before entering the constriction and (b) deformed microgel in the constriction. Schematic models of (c) initial, and (d) deformed particles and (e, f) corresponding POM images.

The ChNC microgel stimuli-responsive behavior further suggests that the structures may possess the ability to deform in a constricted space. Inspired by studies of Doyle and coworkers who showed that the internal structure of a microgel governs its ability to deform in small channel,[58] the impact of the twisted structure on the elastic deformation of ChNC microgels was evaluated. Fig. 4a presents an image of a twisted bipolar microgel (average pitch: 38 μm) in a microfluidic device prior to entering a narrow channel (50 μm). Water flow was generated to guide the microgel into the channel while the process was monitored using POM and high-speed imaging. The long axis of the microgel entered parallel to the passageway (Fig. 4b and Supplementary Video 1). When the long axis of the ChNC microgel was perpendicular to the confined channel, the microgel rotated to possess a favorable configuration (long-axis ∥ passageway) for entering the channel. The outer twisted bands appeared to squeeze by folding on themselves, similar to buckling of a column subjected to axial compression,[59] while the central band forms an angle 'α' with respect to the flow direction. Similar results were found by Doyle, *et al*.[53] for the deformation of particles with internal structure in flow.

Fig. 4c and 4d present schematic models that depict the twisted bipolar microgels without (Fig. 4e) and with constriction (Fig. 4f), respectively. Before entering the passageway, the major and minor axis length was 100 μm and 82 μm, respectively. The angle of twist from the horizontal axis for the band in the center was nearly 90 °; the bend in the center deformed to a 45 ° angle under constriction. The major axis elongated to 114 μm, while the minor axis filled the constriction. After exiting, microgel shape was restored to the original in 3 s (Supplementary Video 2). Deformation of a microgel having a concentric-packing configuration is provided in the in Fig. S13 and Supplementary Video 3. The observed ChNC microgel deformation may provide a

platform for further investigations into how the elastic behavior of Bouligand structures in living organisms contributes to their stress response.

In summary, we demonstrated ChNC microgels that exhibit anisotropic response to external stimuli. The cholesteric texture directly influenced microgel shape and anisotropy in water, and changes in microgel volume led to changes in texture. Specifically, a twisted bipolar texture was discerned in microgels comprising up to 6 bands, while those with greater volumes exhibited concentric-packing. The transition was explained by interplay of anchoring and elastic energy, suggested from thermotropic LC models. As designed, the imprinted cholesteric phase induced an asymmetric response to temperature, leading to a change in shape and optical properties. Furthermore, the cholesteric structure can deform, facilitating transport into a small channel, which is expected to contribute to future studies aimed at evaluating the elastic modulus of Bouligand structures and response to mechanical stress. Access to synthetic structures having self-assembled twisted texture derived from cholesterics embedded within a polymer matrix will provide guidelines for designing biopolymer composites with programmable motion.

Acknowledgements: The authors would like to acknowledge the National Science Foundation Grant No. 1939289 for financial support. This work was performed in part at the Georgia Tech Institute for Electronics and Nanotechnology, a member of the National Nanotechnology Coordinated Infrastructure, which is supported by the National Science Foundation (ECCS-1542174). E.R. appreciates support associated with Carl Robert Anderson Chair funds at Lehigh University. The authors also thank Dr. Brian Khau for fabrication of the Si master used for PDMS device fabrication.

The Supporting Information:

Experimental methods, supporting data, and photographs (PDF)

Supplementary Video 1: Twisted bipolar microgel under constriction (AVI)

Supplementary Video 2: Restoring shape of the microgel (AVI)

Supplementary Video 3: Concentric layered microgel under constriction (AVI)

Funding: This work is supported by a grant from National Science Foundation (1939289).

Competing interests: The authors declare no competing financial interests.

Data and materials availability: All the data needed to evaluate the conclusions of this paper are presented in the paper and/or the Supplementary Materials. Additional data related to this paper can be requested from the authors.

References:

1. Bouligand, Y., Twisted Fibrous Arrangements in Biological-Materials and Cholesteric Mesophases. *Tissue Cell* **1972,** *4* (2), 189-217.

2. Mitov, M., Cholesteric liquid crystals in living matter. *Soft Matter* **2017,** *13* (23), 4176-4209.

3. Natarajan, B.; Gilman, J., Bioinspired Bouligand cellulose nanocrystal composites: a review of mechanical properties. *Philos T R Soc A* **2018,** *376* (2112), 20170050.

4. Bouligand, Y., Sur Une Architecture Torsadee Repandue Dans De Nombreuses Cuticules Darthropodes. *Cr Hebd Acad Sci* **1965,** *261* (18), 3665-3668.

5. Sharma, V.; Crne, M.; Park, J. O.; Srinivasarao, M., Bouligand Structures Underlie Circularly Polarized Iridescence of Scarab Beetles: A Closer View. *Mater Today-Proc* **2014,** *1*, 161-171.

6. Sharma, V.; Crne, M.; Park, J. O.; Srinivasarao, M., Structural Origin of Circularly Polarized Iridescence in Jeweled Beetles. *Science* **2009,** *325* (5939), 449-451.

7. Zhang, C. Q.; Mcadorns, D. A.; Grunion, J. C., Nano/Micro-Manufacturing of Bioinspired Materials: a Review of Methods to Mimic Natural Structures (vol 28, pg 6292, 2016). *Adv Mater* **2016,** *28* (39), 8566-8566.

8. Yang, Y.; Chen, Z. Y.; Song, X.; Zhang, Z. F.; Zhang, J.; Shung, K. K.; Zhou, Q. F.; Chen, Y., Biomimetic Anisotropic Reinforcement Architectures by Electrically Assisted Nanocomposite 3D Printing. *Advanced Materials* **2017,** *29* (11), 1605750.

9. Grunenfelder, L. K.; Herrera, S.; Kisailus, D., Crustacean-Derived Biomimetic Components and Nanostructured Composites. *Small* **2014,** *10* (16), 3207-3232.

10. Rey, A. D., Liquid crystal models of biological materials and processes. *Soft Matter* **2010,** *6* (15), 3402-3429.

11. Shim, T. S.; Kim, S. H.; Heo, C. J.; Jeon, H. C.; Yang, S. M., Controlled Origami Folding of Hydrogel Bilayers with Sustained Reversibility for Robust Microcarriers. *Angew Chem Int Edit* **2012,** *51* (6), 1420-1423.

12. Yao, C.; Liu, Z.; Yang, C.; Wang, W.; Ju, X. J.; Xie, R.; Chu, L. Y., Smart Hydrogels with Inhomogeneous Structures Assembled Using Nanoclay-Cross-Linked Hydrogel Subunits as Building Blocks. *Acs Appl Mater Inter* **2016,** *8* (33), 21721-21730.

13. Zheng, W. J.; An, N.; Yang, J. H.; Zhou, J. X.; Chen, Y. M., Tough Al-alginate/Poly(N-isopropylacrylamide) Hydrogel with Tunable LCST for Soft Robotics. *Acs Appl Mater Inter* **2015,** *7* (3), 1758-1764.

14. Yao, C.; Liu, Z.; Yang, C.; Wang, W.; Ju, X. J.; Xie, R.; Chu, L. Y., Poly(N-isopropylacrylamide)-Clay Nanocomposite Hydrogels with Responsive Bending Property as Temperature-Controlled Manipulators. *Adv Funct Mater* **2015,** *25* (20), 2980-2991.

15. Asoh, T. A.; Matsusaki, M.; Kaneko, T.; Akashi, M., Fabrication of temperature-responsive bending hydrogels with a nanostructured gradient. *Advanced Materials* **2008,** *20* (11), 2080-2083.

16. Le, X. X.; Zhang, Y. C.; Lu, W.; Wang, L.; Zheng, J.; Ali, I.; Zhang, J. W.; Huang, Y. J.; Serpe, M. J.; Yang, X. T.; Fan, X. D.; Chen, T., A Novel Anisotropic Hydrogel with Integrated Self-Deformation and Controllable Shape Memory Effect. *Macromol Rapid Comm* **2018,** *39* (9).

17. Liu, Y.; Takafuji, M.; Ihara, H.; Zhu, M. F.; Yang, M. S.; Gu, K.; Guo, W. L., Programmable responsive shaping behavior induced by visible multi-dimensional gradients of magnetic nanoparticles (vol 8, pg 3295, 2012). *Soft Matter* **2013,** *9* (48), 11706-11706.

18. Ko, J.; Kim, D.; Song, Y.; Lee, S.; Kwon, M.; Han, S.; Kang, D.; Kim, Y.; Huh, J.; Koh, J. S.; Cho, J., Electroosmosis-Driven Hydrogel Actuators Using Hydrophobic/Hydrophilic Layer-By-Layer Assembly-Induced Crack Electrodes. *Acs Nano* **2020,** *14* (9), 11906-11918.

19. Zhu, Z. C.; Senses, E.; Akcora, P.; Sukhishvili, S. A., Programmable Light-Controlled Shape Changes in Layered Polymer Nanocomposites. *Acs Nano* **2012,** *6* (4), 3152-3162.

20. Shi, W.; Huang, J.; Fang, R. C.; Liu, M. J., Imparting Functionality to the Hydrogel by Magnetic-Field-Induced Nano-assembly and Macro-response. *Acs Appl Mater Inter* **2020,** *12* (5), 5177-5194.

21. Wu, L. L.; Ohtani, M.; Takata, M.; Saeki, A.; Seki, S.; Ishida, Y.; Aida, T., Magnetically Induced Anisotropic Orientation of Graphene Oxide Locked by in Situ Hydrogelation. *Acs Nano* **2014,** *8* (5), 4640-4649.

22. Liu, K. Z.; Han, L.; Tang, P. F.; Yang, K. M.; Gan, D. L.; Wang, X.; Wang, K. F.; Ren, F. Z.; Fan, L. M.; Xu, Y. G.; Lu, Z. F.; Lu, X., An Anisotropic Hydrogel Based on Mussel-Inspired Conductive Ferrofluid Composed of Electromagnetic Nanohybrids. *Nano Letters* **2019,** *19* (12), 8343-8356.

23. Odent, J.; Vanderstappen, S.; Toncheva, A.; Pichon, E.; Wallin, T. J.; Wang, K. Y.; Shepherd, R. F.; Dubois, P.; Raquez, J. M., Hierarchical chemomechanical encoding of multi-responsive hydrogel actuators via 3D printing. *J Mater Chem A* **2019,** *7* (25), 15395-15403.

24. Arslan, H.; Nojoomi, A.; Jeon, J.; Yum, K., 3D Printing of Anisotropic Hydrogels with Bioinspired Motion. *Advanced Science* **2019,** *6* (2).

25. Gladman, A. S.; Matsumoto, E. A.; Nuzzo, R. G.; Mahadevan, L.; Lewis, J. A., Biomimetic 4D printing. *Nat Mater* **2016,** *15* (4), 413-418.

26. Lee, K. Y.; Mooney, D. J., Hydrogels for tissue engineering. *Chem Rev* **2001,** *101* (7), 1869-1879.

27. Huang, G. Y.; Li, F.; Zhao, X.; Ma, Y. F.; Li, Y. H.; Lin, M.; Jin, G. R.; Lu, T. J.; Genin, G. M.; Xu, F., Functional and Biomimetic Materials for Engineering of the Three-Dimensional Cell Microenvironment. *Chem Rev* **2017,** *117* (20), 12764-12850.

28. Yasuda, K.; Kitamura, N.; Gong, J. P.; Arakaki, K.; Kwon, H. J.; Onodera, S.; Chen, Y. M.; Kurokawa, T.; Kanaya, F.; Ohmiya, Y.; Osada, Y., A Novel Double-Network Hydrogel Induces Spontaneous Articular Cartilage Regeneration in vivo in a Large Osteochondral Defect. *Macromol Biosci* **2009,** *9* (4), 307-316.

29. Peppas, N. A.; Hilt, J. Z.; Khademhosseini, A.; Langer, R., Hydrogels in biology and medicine: From molecular principles to bionanotechnology. *Adv Mater* **2006,** *18* (11), 1345-1360.

30. Calvert, P., Hydrogels for Soft Machines. *Adv Mater* **2009,** *21* (7), 743-756.

31. Ionov, L., Biomimetic Hydrogel-Based Actuating Systems. *Adv Funct Mater* **2013,** *23* (36), 4555-4570.

32. Yu, C. J.; Duan, Z.; Yuan, P. X.; Li, Y. H.; Su, Y. W.; Zhang, X.; Pan, Y. P.; Dai, L. L.; Nuzzo, R. G.; Huang, Y. G.; Jiang, H. Q.; Rogers, J. A., Electronically Programmable, Reversible Shape Change in Two- and Three-Dimensional Hydrogel Structures. *Adv Mater* **2013,** *25* (11), 1541-1546.

33. Iwaso, K.; Takashima, Y.; Harada, A., Fast response dry-type artificial molecular muscles with [c2]daisy chains. *Nature Chemistry* **2016,** *8* (6), 626-633.

34. Lee, B. P.; Konst, S., Novel Hydrogel Actuator Inspired by Reversible Mussel Adhesive Protein Chemistry. *Adv Mater* **2014,** *26* (21), 3415-3419.

35. Pei, X. D.; Zan, T. T.; Li, H. M.; Chen, Y. J.; Shi, L. Q.; Zhang, Z. K., Pure Anisotropic Hydrogel with an Inherent Chiral Internal Structure Based on the Chiral Nematic Liquid Crystal Phase of Rodlike Viruses. *Acs Macro Lett* **2015,** *4* (11), 1215-1219.

36. Wu, Z. L.; Kurokawa, T.; Liang, S.; Furukawa, H.; Gong, J. P., Hydrogels with Cylindrically Symmetric Structure at Macroscopic Scale by Self-Assembly of Semi-rigid Polyion Complex. *J Am Chem Soc* **2010,** *132* (29), 10064-10069.

37. Kyle, S.; Aggeli, A.; Ingham, E.; McPherson, M. J., Production of self-assembling biomaterials for tissue engineering. *Trends Biotechnol* **2009,** *27* (7), 423-433.

38. Cho, S. H.; Li, Y. F.; Seo, M.; Kumacheva, E., Nanofibrillar Stimulus-Responsive Cholesteric Microgels with Catalytic Properties. *Angew Chem Int Edit* **2016,** *55* (45), 14014-14018.

39. Wang, P. X.; Hamad, W. Y.; MacLachlan, M. J., Polymer and Mesoporous Silica Microspheres with Chiral Nematic Order from Cellulose Nanocrystals. *Angew Chem Int Edit* **2016,** *55* (40), 12460-12464.

40. Peng, N.; Huang, D.; Gong, C.; Wang, Y. X.; Zhou, J. P.; Chang, C. Y., Controlled Arrangement of Nanocellulose in Polymeric Matrix: From Reinforcement to Functionality. *Acs Nano* **2020,** *14* (12), 16169-16179.

41. Kelly, J. A.; Shukaliak, A. M.; Cheung, C. C. Y.; Shopsowitz, K. E.; Hamad, W. Y.; MacLachlan, M. J., Responsive Photonic Hydrogels Based on Nanocrystalline Cellulose. *Angew Chem Int Edit* **2013,** *52* (34), 8912-8916.

42. Revol, J. F.; Marchessault, R. H., In-Vitro Chiral Nematic Ordering of Chitin Crystallites. *Int J Biol Macromol* **1993,** *15* (6), 329-335.

43. Li, J.; Revol, J. F.; Naranjo, E.; Marchessault, R. H., Effect of electrostatic interaction on phase separation behaviour of chitin crystallite suspensions. *Int J Biol Macromol* **1996,** *18* (3), 177-187.

44. Marchessault, R. H.; Morehead, F. F.; Walter, N. M., Liquid Crystal Systems from Fibrillar Polysaccharides. *Nature* **1959,** *184* (4686), 632-633.

45. Zhou, Y.; Bukusoglu, E.; Martinez-Gonzalez, J. A.; Rahimi, M.; Roberts, T. F.; Zhang, R.; Wang, X. G.; Abbott, N. L.; de Pablo, J. J., Structural Transitions in Cholesteric Liquid Crystal Droplets. *Acs Nano* **2016,** *10* (7), 6484-6490.

46. Orlova, T.; Asshoff, S. J.; Yamaguchi, T.; Katsonis, N.; Brasselet, E., Creation and manipulation of topological states in chiral nematic microspheres. *Nat Commun* **2015,** *6*, 7603.

47. Miller, D. S.; Wang, X. G.; Abbott, N. L., Design of Functional Materials Based on Liquid Crystalline Droplets. *Chem Mater* **2014,** *26* (1), 496-506.

48. Li, Y. F.; Suen, J. J. Y.; Prince, E.; Larin, E. M.; Klinkova, A.; Therien-Aubin, H.; Zhu, S. J.; Yang, B.; Helmy, A. S.; Lavrentovich, O. D.; Kumacheva, E., Colloidal cholesteric liquid crystal in spherical confinement. *Nat Commun* **2016,** *7*, 12520 .

49. Tixier, T.; Heppenstall-Butler, M.; Terentjev, E. M., Spontaneous size selection in cholesteric and nematic emulsions. *Langmuir* **2006,** *22* (5), 2365-2370.

50. Lin, I. H.; Miller, D. S.; Bertics, P. J.; Murphy, C. J.; de Pablo, J. J.; Abbott, N. L., Endotoxin-Induced Structural Transformations in Liquid Crystalline Droplets. *Science* **2011,** *332* (6035), 1297-1300.

51. Bagnani, M.; Azzari, P.; De Michele, C.; Arcari, M.; Mezzenga, R., Elastic constants of biological filamentous colloids: estimation and implications on nematic and cholesteric tactoid morphologies. *Soft Matter* **2021,** *17* (8), 2158-2169.

52. Pieranski, P.; Godinho, M. H., *Liquid Crystals : New Perspectives*. John Wiley & Sons, Incorporated: Newark, 2021.

53. Sleczkowski, P.; Zhou, Y.; Iamsaard, S.; de Pablo, J. J.; Katsonis, N.; Lacaze, E., Light-activated helical inversion in cholesteric liquid crystal microdroplets. *P Natl Acad Sci USA* **2018,** *115* (17), 4334-4339.

54. Chen, G. H.; Hoffman, A. S., Graft-Copolymers That Exhibit Temperature-Induced Phase-Transitions over a Wide-Range of Ph. *Nature* **1995,** *373* (6509), 49-52.

55. Amiya, T.; Hirokawa, Y.; Hirose, Y.; Li, Y.; Tanaka, T., Reentrant Phase-Transition of N-Isopropylacrylamide Gels in Mixed-Solvents. *J Chem Phys* **1987,** *86* (4), 2375-2379.

56. Schneider, C. A.; Rasband, W. S.; Eliceiri, K. W., NIH Image to ImageJ: 25 years of image analysis. *Nat Methods* **2012,** *9* (7), 671-675.

57. Nikolov, S.; Petrov, M.; Lymperakis, L.; Friak, M.; Sachs, C.; Fabritius, H. O.; Raabe, D.; Neugebauer, J., Revealing the Design Principles of High-Performance Biological Composites Using Ab initio and Multiscale Simulations: The Example of Lobster Cuticle. *Adv Mater* **2010,** *22* (4), 519-526.

58. Chen, L.; Wang, K. X.; Doyle, P. S., Effect of internal architecture on microgel deformation in microfluidic constrictions. *Soft Matter* **2017,** *13* (9), 1920-1928.

59. Gregory, M. S., *Elastic instability: analysis of buckling modes and loads of framed structures*. Spon: London,, 1967; p xii, 354 p.

Table of Contents Graphic (TOC)